Available online at www.sciencedirect.com
ScienceDirect
Trans. Nonferrous Met. Soc. China 34(2024) 2787−2799
Transactions of Nonferrous Metals Society of China
www.tnmsc.cn

# Effect of combination of ultraviolet radiation and biocide on fungal-induced corrosion of high-strength 7075 aluminum alloy

Zheng-yu JIN[#], Chao WANG[#], Hai-xian LIU, Hong-wei LIU

School of Chemical Engineering and Technology, Sun Yat-sen University, Zhuhai 519082, China

Received 11 March 2023; accepted 21 September 2023

**Abstract:** The effect of ultraviolet (UV) radiation and biocide benzalkonium chloride (BKC) on fungal-induced corrosion of AA7075 induced by *Aspergillus terreus* (*A. terreus*) was deeply studied using analysis of biological activity, surface analysis, and electrochemical measurements. Results demonstrated that the planktonic and sessile spore concentrations decline by more than two orders of magnitude when UV radiation and BKC are combinedly used compared with the control. UV radiation can inhibit the biological activity of *A. terreus* and influence the stability of passive film of AA7075. Except for direct disinfection, the physical adsorption of BKC on the specimen can effectively inhibit the attachment of *A. terreus*. The combination of UV radiation and BKC can much more effectively inhibit the corrosion of AA, especially pitting corrosion, due to their synergistic effect. The combined application of UV radiation and BKC can be a good method to effectively inhibit fungal-induced corrosion.

**Key words:** fungal-induced corrosion; *Aspergillus terreus*; 7075 aluminum alloy; ultraviolet radiation; benzalkonium chloride

## 1 Introduction

Aluminum alloys (AA), especially those with high strength, have been commonly applied in various industrial fields, such as the aviation industry, because of their low-density, favorable mechanical performance as well as high corrosion resistance [1,2]. However, AA can still suffer from severe localized corrosion in harsh marine environments [3,4], including pitting corrosion [5], stress corrosion cracking [6], and microbiologically influenced corrosion (MIC) [7]. MIC often results in corrosion acceleration by affecting the corrosion kinetics or modifying the chemical composition of the protective film. MIC has a hugely destructive effect on engineering materials, and it is regarded as one of the primary factors causing the corrosion acceleration of AA in marine environments. Many corrosive microorganisms in natural environments, including sulfate-reducing bacteria (SRB), fungi, and microalgae, can significantly enhance AA corrosion [8−10]. Currently, fungi have been found as one of the typical corrosive microorganisms which are responsible for AA corrosion. JIRÓN-LAZOS et al [11] discovered that *Aspergillus niger*, the typical fungi, promoted the formation of a differential aeration corrosion cell, and thus resulting in the localized corrosion of AA 6061. The authors' previous work [12] demonstrated that fungus *Aspergillus terreus* could grow well and form a biofilm on AA7075 even if the organic carbon source was deficient, and it helps to destroy the passive film of AA, causing the occurrence of severe pitting corrosion. Fungi can usually secret amounts of organic acids, leading to the decrease of pH value of the test solution, so acid corrosion is also regarded as a potential factor accelerating AA

[#]Zheng-yu JIN and Chao WANG contributed equally to this work

**Corresponding author:** Hong-wei LIU, E-mail: liuhw35@mail.sysu.edu.cn

DOI: 10.1016/S1003-6326(24)66576-3

corrosion [7,13]. The possible electron transfer from AA to fungi can also significantly accelerate AA corrosion, especially for localized corrosion. Even though researchers have done much work to investigate AA corrosion behavior caused by fungi, the fungal-induced corrosion mechanism is still unclear and detailed studies are essential.

The investigations of corrosion mechanism are the basis to do corrosion protection. Currently, biocides are widely adopted to control MIC by directly killing microorganisms [14−16]. Although the use of biocides is an effective method for inhibiting MIC, the application of large amounts of biocides gives a big threat to environmental protection because of their high toxicity [17,18]. Furthermore, the long-term use of the application can increase antimicrobial resistance, leading to a fast decrease in MIC control efficiency [19]. Therefore, the future application of biocides in MIC control fields faces some challenges. It is a good idea to decrease the secondary pollution of biocides to the environment by cutting down the used concentration. Biocide enhancers, such as *D*-methionine, can effectively improve the antibacterial efficiency of biocides and decrease the concentration of biocides but without changing anti-MIC efficiency [20,21].

Except for the biocide enhancers, ultraviolet (UV) radiation can also possibly increase the antibacterial efficiency of biocides. UV radiation is also a comment method used to sterilize materials because it can induce DNA damage to cells [22,23]. It is found that UV radiation has a corrosion inhibition effect on metals [24,25]. Furthermore, some researchers found that UV radiation can be a good and eco-friendly method for MIC protection [26]. Therefore, the combination of UV radiation and biocides can be an ideal choice to control MIC by significantly increasing MIC inhibition efficiency. This is also helpful to decrease the used concentration of biocides due to their combined action. The protective effects of UV radiation and biocides can be better if the biocides have some corrosion inhibition effects. The combination of UV radiation and biocides is also helpful to decrease the applied intensity of UV radiation. However, deep studies of the combined effects of UV radiation and biocides are still absent.

In this work, the effect of the combination of UV radiation and biocide on the corrosion of high-strength AA7075 in 3.5 wt.% NaCl solution containing *Aspergillus terreus* (*A. terreus*) was deeply investigated based on electrochemical measurements and surface analysis, such as electrochemical impedance spectroscopy (EIS), potentiodynamic and potentiostatic polarization curves, scanning electron microscopy (SEM), and X-ray photoelectron spectrometer (XPS). Benzalkonium chloride (BKC), the typical biocide, was applied, and BKC is also a corrosion inhibitor having a good corrosion inhibition effect in abiotic conditions [27]. This work aims to provide a deep understanding of the synergistic inhibition effect between UV radiation and BKC for the fungal-induced corrosion of AA in the presence of *A. terreus*.

## 2 Experimental

### 2.1 Preparation of specimens

AA7075 with a high strength was used in this work, and its chemical components were composed (wt.%) of Zn 6.00, Mg 2.40, Cu 2.50, Si 0.40, Mn 0.30, Fe 0.50, Ti 0.20, Cr 0.18, and Al balance. For surface analysis and electrochemical measurements, the specimens of 10 mm × 10 mm × 10 mm were prepared. Only the working face was reserved corresponding to a working area of 1 $cm^2$, and the other faces were coated with epoxy resin. Prior to use, specimens were polished with grit silicon carbide papers of grades $400^{\#}$, $600^{\#}$, $800^{\#}$, and $1200^{\#}$. After polishing, all specimens were successively washed with acetone and then anhydrous ethanol, and dried in $N_2$. The reference electrode, AA specimens and counter electrode were sterilized under UV irradiation for more than 30 min to avoid the influence of miscellaneous bacteria on MIC study.

### 2.2 Fungi cultivation and inoculation

*A. terreus*, a typical corrosive fungus isolated from the South China Sea, was chosen for the corrosion study [12]. The fresh medium applied to culturing *A. terreus* was a potato-dextrose agar containing NaCl of 30 g/L, glucose of 20 g/L, and potato infusion of 200 mL/L. The culture medium of *A. terreus* was firstly autoclaved at 121 °C for 20 min before use. After sterilization, *A. terreus* was inoculated in the prepared culture medium, and was incubated at 37 °C. The biological activity of

*A. terreus* depended on the changes in the counts of planktonic and sessile spores, and spores were counted by a plate count method.

### 2.3 Test solution

The test solution was composed of 3.5 wt.% NaCl solution and 10 wt.% sterilized culture medium of *A. terreus*. And the addition of 10 wt.% sterilized culture medium aimed to improve the biological activity of *A. terreus* by promoting its growth. The abiotic test solution was the control. The test solution was sterilized at 121 °C for 20 min before tests. The solution volume was 300 mL in a test vial of 520 mL. BKC with a low concentration of 20 mg/L was added to the test solution.

### 2.4 Characterization of surface morphologies

SEM and EDS (JSM-IT200, JEOL, Japan) were used to characterize the structure and components of surface biofilms as well as the bare morphologies of pitting corrosion. Prior to SEM observation of biofilm, the specimens were pretreated after taking out from the test solution on the 21st day. The pretreatment was the fixation of biofilm in phosphate buffer solution containing 2.5 wt.% glutaraldehyde. And the fixed time was 8 h to completely kill *A. terreus*. Then, these specimens were dehydrated with a series of ethanol solutions (30%, 50%, 70%, and 100%), and each concentration was 15 min. After dehydration, all specimens were dried in $N_2$. After pretreatment, a thin gold film was coated on specimens to significantly improve the electrical conductivity of biofilm.

### 2.5 Electrochemical measurements

Open-circuit potential (OCP), EIS, potentiodynamic and potentiostatic polarization curves were measured by an electrochemical workstation (CS350H, Corrtest, China). A three-electrode cell was constructed while AA specimen, saturated calomel electrode (SCE) and platinum plate corresponding to the working electrode, reference electrode and counter electrode, respectively. A UV light with a power of 8 W was used, and its intensity was 28 μW/cm$^2$. The UV light had a wavelength of 253.7 nm. The distance between UV light and test vial was set as 20 cm, and the surface of the specimen was perpendicular to UV light so that UV light can directly radiate the specimen surface. OCP was first monitored prior to EIS measurements. EIS was scanned by applying a sinusoidal wave of 10 mV, and the selective frequency ranged from $10^5$ to $10^{-2}$ Hz. Potentiodynamic polarization tests with a potential scanning range from −0.25 to 0.5 V (vs OCP) were performed on the 21st day following the EIS measurements. The potential scanning rate was set as 0.5 mV/s. The potentiostatic polarization curves were measured at −0.7 V (vs SCE) using independent specimens.

## 3 Results

### 3.1 Spore counts of *A. terreus*

Figure 1 shows the changes in the biological activity of *A. terreus* before and after 21 d of testing based on the counts of planktonic and sessile spores. The original spore concentrations of *A. terreus* for all test conditions are same with a value of about $10^8$ spores/mL. The specimen in the absence of BKC and UV radiation is used as the control. After 21 d, the spore counts of sessile and planktonic *A. terreus* for the control specimen are $1\times10^8$ spores/cm$^2$ and $7.7\times10^7$ spores/mL, respectively. These suggest that *A. terreus* can survive well in the test solution and form a biofilm on the specimen surface. Both the spore concentrations of planktonic and sessile *A. terreus* decrease by an order of magnitude when UV radiation or BKC are individually applied compared with the control. Therefore, UV radiation and BKC both have some

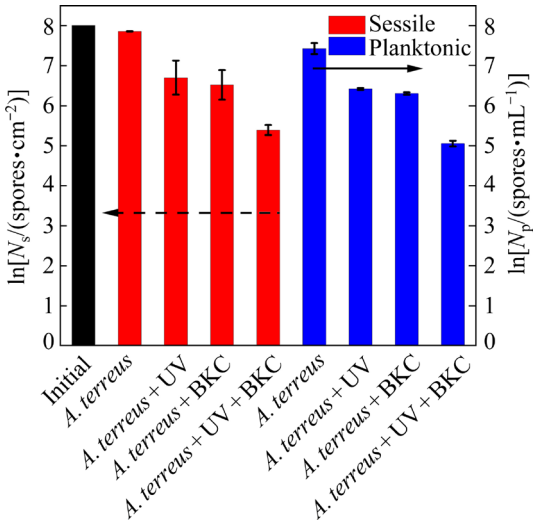


**Fig. 1** Planktonic and sessile spore counts showing biological activity of *A. terreus* after 21 d of testing

inhibition effect on the growth of *A. terreus*, but the antifungal effect of BKC is better than UV radiation when they are singly used. However, their antifungal effects are not better because the intensity of UV radiation and the concentration of BKC both are low. Furthermore, it is found that the concentrations of both planktonic and sessile spores decline by more than two orders of magnitude when UV radiation and BKC are used in combination. At this moment, the sessile and planktonic spore counts of *A. terreus* reach $5.4\times10^5$ spores/cm$^2$ and $1\times10^5$ spores/mL, respectively. Therefore, the combination of UV radiation and BKC has a synergistic antifungal effect on *A. terreus* from the changes in the biological activities of *A. terreus*.

### 3.2 Biofilm characteristics

SEM images of the formed biofilms by *A. terreus* after 21 d immersion in 3.5 wt.% NaCl solution under various test conditions are presented in Fig. 2. For the control specimen, i.e., no application of UV radiation and BKC, it is seen that a biofilm is formed on the specimen containing a large number of hyphae and spores, and the distribution of biofilm is homogeneous (Figs. 2(a, b)), suggesting the good growth and high metabolic activity of *A. terreus*. As a comparison, only some amounts of hyphae and spores mixed with corrosion products are observed on the specimen when UV radiation is individually applied (Figs. 2(d, e)). But the biofilm in the presence of UV radiation is heterogeneous. Compared

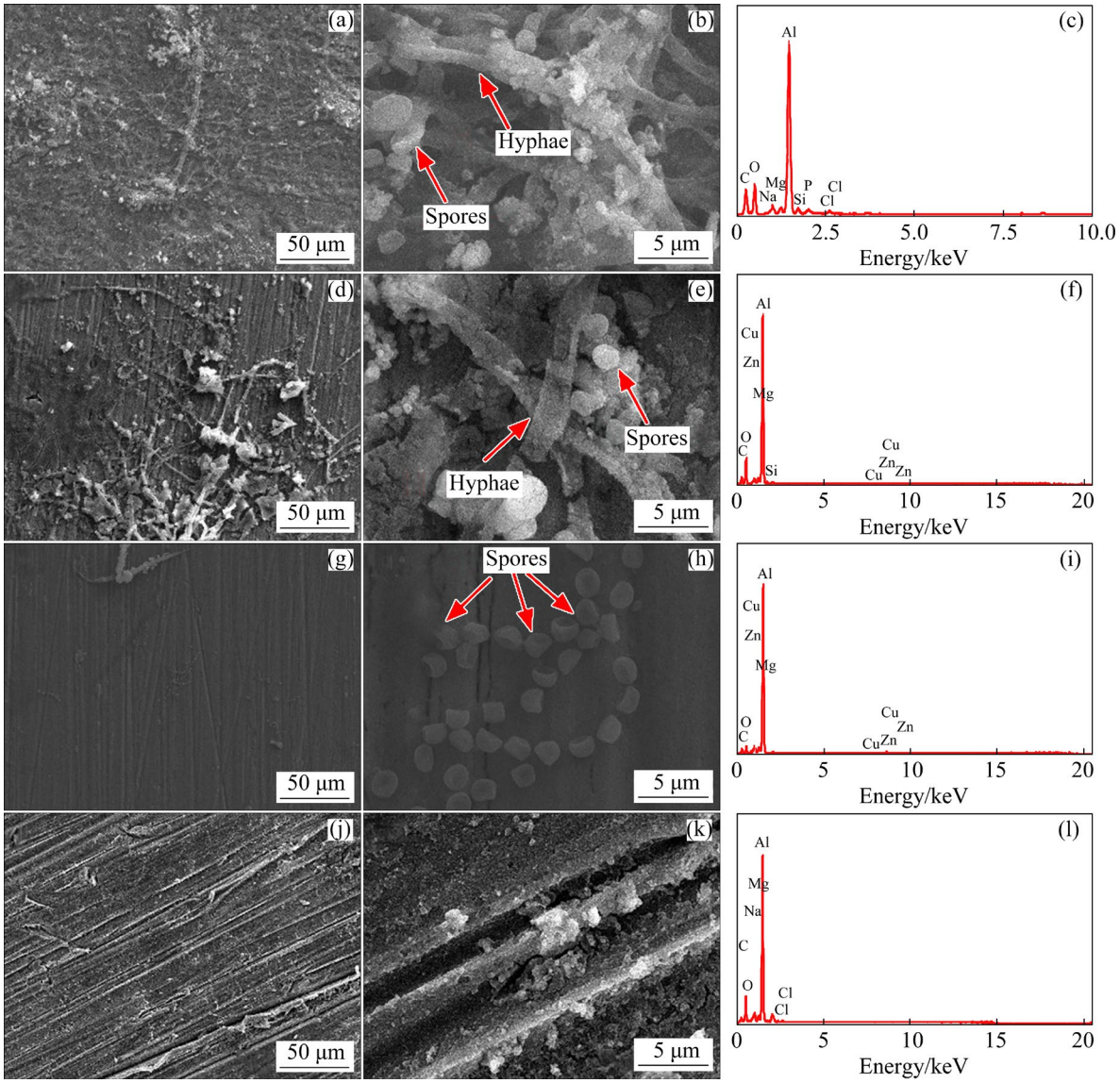


**Fig. 2** SEM images of surface films in the presence of *A. terreus* after 21 d immersion in 3.5 wt.% NaCl solution under different test conditions: (a, b, c) *A. terreus* (control); (d, e, f) *A. terreus* + UV radiation; (g, h, i) *A. terreus* + BKC; (j, k, l) *A. terreus* + UV radiation + BKC

with the control, the presence of UV radiation surely inhibits the adhesion of *A. terreus* as well as the subsequent biofilm formation. When 20 mg/L BKC is added to the test solution, it is difficult for the adhesion of *A. terreus* on the surface of the specimen, and only a low number of hyphae and spores cover the specimen surface (Figs. 2(g, h)). Therefore, AA corrosion can be slight in the presence of BKC. However, when UV radiation and BKC are combinedly used, almost no hyphae and spores can be found on the specimen and slight corrosion is also seen (Figs. 2(j, k)). Compared with the absence or individually used UV radiation and BKC, it is easily recognized that there is a synergistic effect inhibiting the adhesion and the subsequent formation of fungi biofilm when UV radiation and BKC are applied simultaneously. EDS results also show that the mass fraction of elements C and O has a decrease in the presence of UV radiation and BKC no matter whether they are individually or combinedly used.

### 3.3 Pitting corrosion morphology

After 21 d of testing, the corrosion products are removed, and the bare surface morphologies of the specimens under different test conditions are presented in Fig. 3. It is found that the severe pitting corrosion of the control specimen caused by *A. terreus* can be observed (Figs. 3(a, b)). And some corrosion pits are also recognized (Fig. 3(a)). Pitting corrosion is the typical corrosion type of AA, especially in the presence of fungi [28,29]. Therefore, *A. terreus* with good biological activity can easily accelerate the pitting corrosion of AA. Some small corrosion pits are also observed in the presence of UV radiation or BKC individually (Figs. 3(c−f)). The formation of corrosion pits is caused by *A. terreus* because of the survival and growth of *A. terreus* in the presence of UV radiation or BKC. However, both the UV radiation and BKC can effectively decline the pitting corrosion induced by *A. terreus* compared with the control. Furthermore, there are no legible corrosion pits when UV radiation and BKC appear simultaneously. Therefore, the combination of UV radiation and BKC can effectively decrease the pitting corrosion of the specimen induced by *A. terreus*, suggesting that UV radiation and BKC have a synergistic corrosion inhibition effect for AA.

### 3.4 XPS spectra of surface films

Figure 4 presents the high-resolution XPS spectra and the corresponding analysis results of C 1s, Al 2p, O 1s, Zn 2p and N 1s for the specimens under various test conditions in 3.5 wt.% NaCl solution after 21 d of testing. For the C 1s spectra, C—H, C═O, O—C—O and C—N functional groups can be found for all specimens corresponding to the organic components of biofilm caused by *A. terreus* (Fig. 4(a)). From Al 2p spectra (Fig. 4(b)), it is seen that the peak located at 74.3 eV is assigned to $Al(OH)_3$ [30], and the peaks at 74.6 and 74.8 eV correspond to $Al_2O_3$ [31]. Therefore, $Al(OH)_3$ and $Al_2O_3$ are the main corrosion products of AA that are formed by *A. terreus*, and the species of corrosion products are similar under different test conditions. In the O 1s spectra (Fig. 4(c)), $Al(OH)_3$ corresponds to the peak

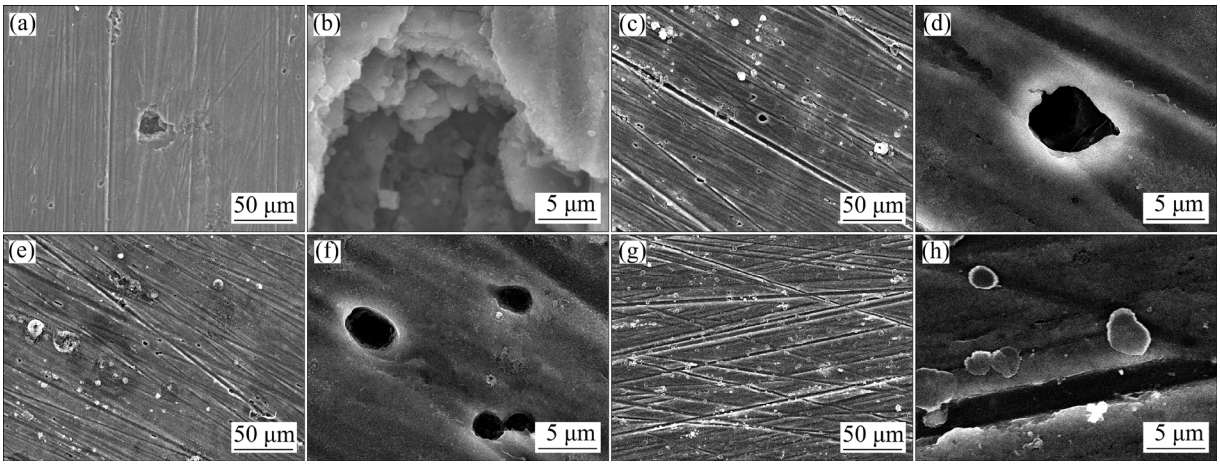


**Fig. 3** SEM images showing surface morphologies of specimens after removing corrosion products after 21 d immersion in 3.5 wt.% NaCl solution containing *A. terreus* under different test conditions: (a, b) *A. terreus*; (c, d) *A. terreus* + UV radiation; (e, f) *A. terreus* + BKC; (g, h) *A. terreus* + UV radiation + BKC

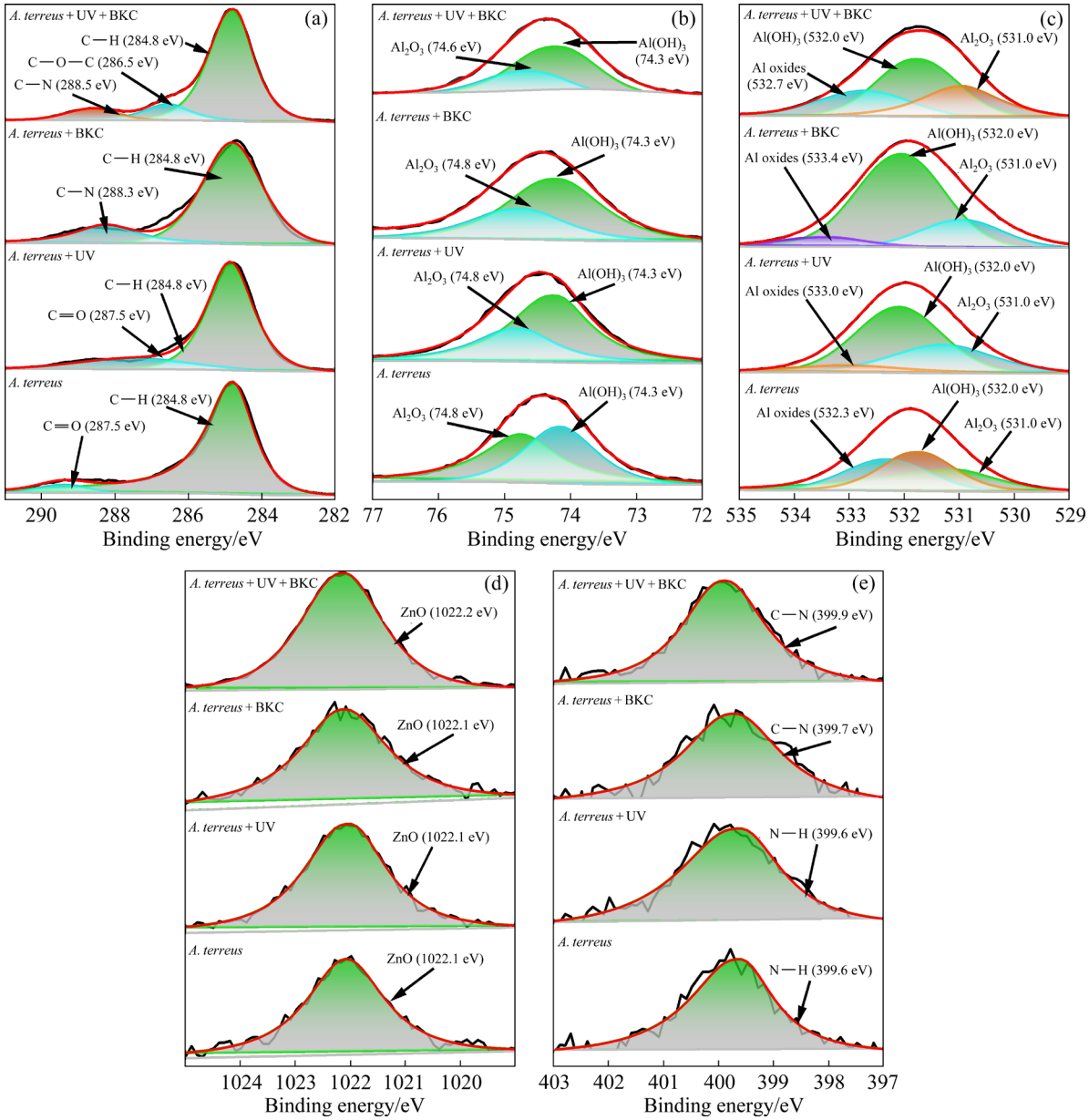


**Fig. 4** High-resolution XPS spectra of C 1s (a), Al 2p (b), O 1s (c), Zn 2p (d), and N 1s (e) for specimens in the presence of *A. terreus* under different test conditions after 21 d immersion in 3.5 wt.% NaCl solution

located at 532.0 eV, and the other peak at 531.0 eV belongs to $Al_2O_3$ [32,33]. Furthermore, some peaks located at 532.3, 532.7, 533.0 and 533.4 eV are assigned to Al oxides (Fig. 4(c)). For Zn 2p spectra, the presence of ZnO corresponding to the peak at 1022.1 eV is seen [3,34]. The presence of ZnO suggests part destruction of the AA passive film. In N 1s spectra, the peak at 399.6 eV in the absence and presence of UV radiation belongs to N—H functional group which can be attributed to the components of organics in biofilm (Fig. 4(e)). There is a peak at 399.9 eV belonging to C—N functional group due to presence of BKC (Fig. 4(e)). The C—N functional group is the typical functional group of BKC, and the appearance of C—N functional group demonstrates the adsorption of BKC on the specimen. BKC as a corrosion inhibitor owns a good inhibition effect in abiotic conditions, which can be conducive to the decrease of AA corrosion rate.

### 3.5 Electrochemical characteristics

#### 3.5.1 OCP results

The changes of OCP of the specimens in the presence of *A. terreus* with time under different conditions in 3.5 wt.% NaCl solution are presented

in Fig. 5. As a comparison with the control specimen, the presence of UV radiation or BKC promotes the positive shift of OCP overall. When UV radiation and BKC are combined, the OCP values are much more positive. Therefore, no matter UV radiation and BKC are individually or combinedly applied, the fungal-induced corrosion tendency of AA induced by *A. terreus* has a decrease.

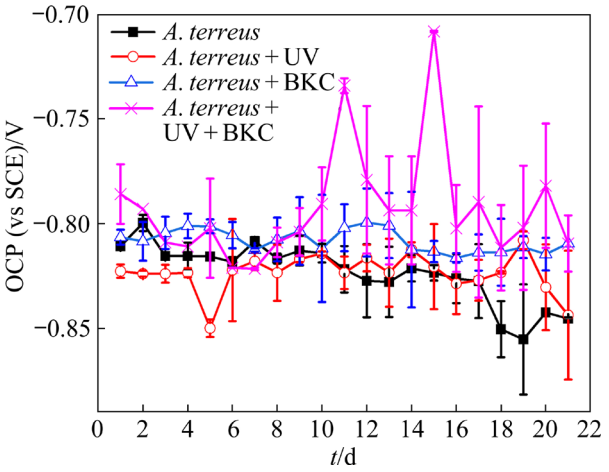


**Fig. 5** Changes of OCP of specimens in the presence of *A. terreus* under different corrosion conditions with time in 3.5 wt.% NaCl solution

3.5.2 EIS analysis results

EIS test was performed following a stable OCP to investigate the fungal-induced corrosion behavior of AA induced by *A. terreus* under various corrosion conditions, and the results are presented in Fig. 6. It shows that the diameters of Nyquist plots in the presence of *A. terreus* change little during the initial 7 d but with small values, suggesting severe corrosion deriving from *A. terreus* (Fig. 6(a)). The presence of inductive impedance can be due to the adsorption of metabolic intermediates secreted by *A. terreus* on electrodes (Fig. 6(a)). The diameters of Nyquist plots turn to be the smallest on the 10th day, and then keep a stable state from the 14th to the 21st day (Fig. 6(a)). The Bode plots in Fig. 6(b) suggest that the passive film has a process of damage and repair, and the damage is probably resulted by *A. terreus*. When the UV radiation is applied, the diameters of Nyquist plots show an increase in comparison with the control, indicating that UV radiation can inhibit the fungal-induced corrosion (Fig. 6(c)). Furthermore, the diameters are small in the original 2 d, but turn to be large over time (Fig. 6(c)). This demonstrates that corrosion inhibition of AA caused by UV radiation will suffer from a long time. For the specimen with the appearance of BKC, the diameters of Nyquist plots are also higher than those of the control specimen, suggesting that the addition of BKC can also inhibit the corrosion of AA7075 induced by *A. terreus* (Fig. 6(e)). Furthermore, the Bode plots with wide phase angles also demonstrate that the AA passive film has favorable stability due to the application of BKC (Fig. 6(f)). However, the diameters of Nyquist plots show the significant improvement when the UV radiation and BKC are applied simultaneously (Fig. 6(g)) in comparison to additional test conditions. This suggests that the combination of UV radiation and BKC is effective to inhibit AA corrosion due to their synergistic effect. Furthermore, a new phase angle appears in the area of low frequency (red circle in Fig. 6(h)), also showing good adsorption of BKC on specimens.

EIS diagrams are fitted using a proper equivalent circuit in Fig. 7. In the meantime, the corresponding fitted results are presented in Fig. 8. In the electrochemical equivalent circuits, electrochemical parameters of $R_s$, $R_f$ and $R_{ct}$ are assigned to the resistances of solution, biofilm, and charge transfer, respectively, while $Q_f$ and $Q_{dl}$ correspond to the capacitances of biofilm and double-layer. Furthermore, $L$, the inductive element, is applied, and $R_L$ represents its resistance. The fitted $R_p$ values correspond to the sum of $R_f$ and $R_{ct}$, which can be used to do the quantitative analysis of AA corrosion rate. A higher $R_p$ value indicates a lower corrosion rate. The changes of $R_p$ values with time fitted from the EIS data using an electrochemical equivalent circuit are shown in Fig. 8. Generally, $R_p$ values are inversely proportional to the corrosion rates, and the lower $R_p$ values, the higher corrosion rates. Figure 8 shows that the $R_p$ values of the control specimen caused by *A. terreus* only are the smallest, demonstrating the highest corrosion rate due to its high corrosivity for AA. When BKC is applied, the $R_p$ values of the specimen increase, suggesting that BKC can inhibit AA corrosion induced by *A. terreus*. Furthermore, the action of BKC is fast due to the high $R_p$ values during the initial 2 d. The $R_p$ values of the specimen after the application of UV radiation have a gradual increase during the initial 7 d, which indicates that UV radiation can inhibit AA corrosion induced by

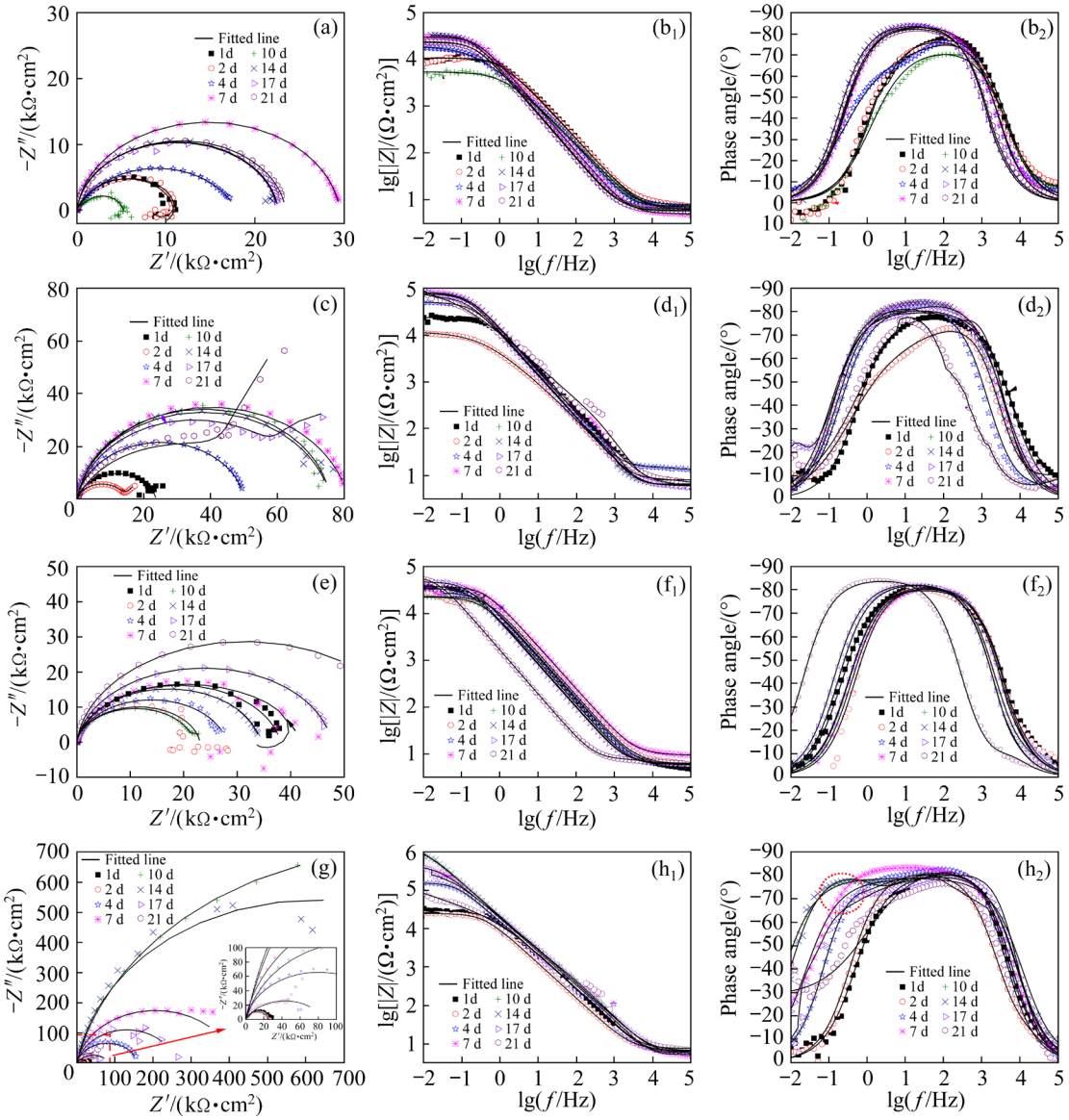


**Fig. 6** Time-dependence of Nyquist (a, c, e, g) and Bode ($b_1$, $b_2$, $d_1$, $d_2$, $f_1$, $f_2$, $h_1$, $h_2$) plots of specimens under different test conditions in 3.5 wt.% NaCl solution: (a, $b_1$, $b_2$) *A. terreus*; (c, $d_1$, $d_2$) *A. terreus* + UV radiation; (e, $f_1$, $f_2$) *A. terreus* + BKC; (g, $h_1$, $h_2$) *A. terreus* + UV radiation + BKC

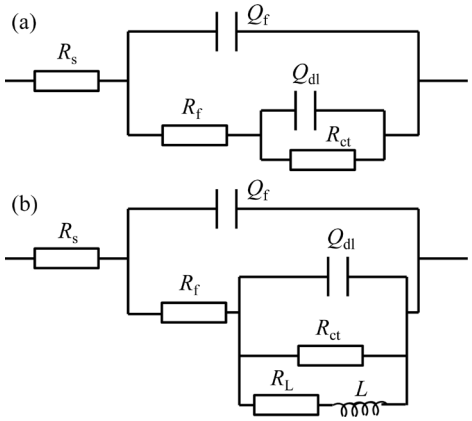


**Fig. 7** Equivalent circuits used to fit experimental impedance diagrams in Fig. 6: (a) Two time-constants; (b) With inductive reactance

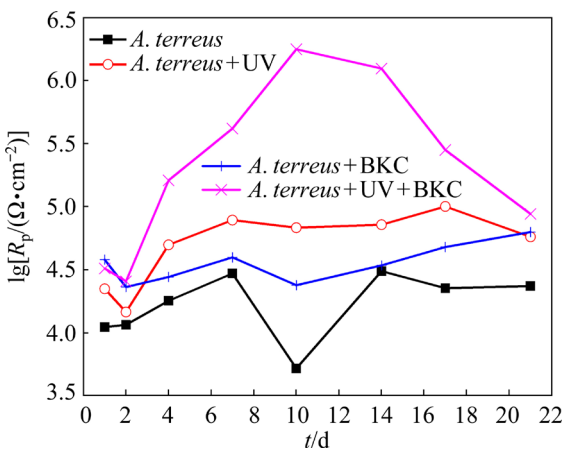


**Fig. 8** Changes of electrochemical parameter $R_p$ fitted from EIS data in Fig. 6 with time

*A. terreus* but spend a long time. However, the $R_p$ values of the specimen have a significant increase with time after the combined use of UV radiation and BKC. Therefore, the corrosion rate of AA is the lowest due to the combination of UV radiation and BKC, i.e., UV radiation and BKC show a synergistic inhibition effect on fungal-induced corrosion of AA.

3.5.3 Potentiodynamic polarization curves

The potentiodynamic polarization curves of specimens in 3.5 wt.% NaCl solution containing *A. terreus* under different test conditions after 21 d of testing are presented in Fig. 9. The corrosion potentials of specimens shift to the positive direction whether the single or combined use of UV radiation and BKC is performed. The cathodic oxygen-reduction reaction is gradually inhibited following the order of UV radiation, BKC, and UV radiation and BKC, while the anodic reaction changes little. Therefore, the application of UV radiation, BKC, and UV radiation and BKC mainly inhibit the cathodic reaction, leading to the decrease of corrosion rates.

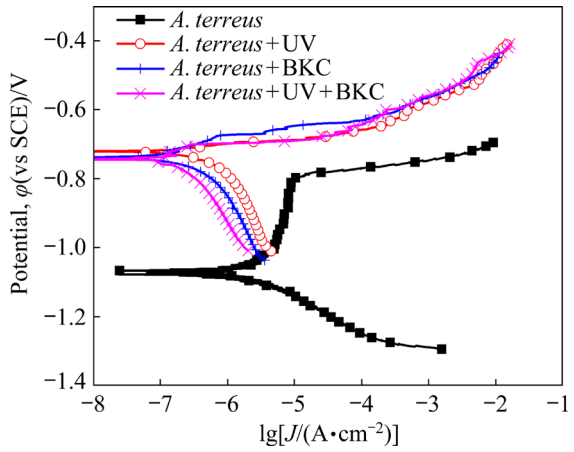


**Fig. 9** Potentiodynamic polarization curves of specimens under different test conditions in 3.5 wt.% NaCl solution containing *A. terreus* after 21 d of testing

3.5.4 Potentiostatic polarization curves

To investigate the effects of UV radiation or BKC on the anodic dissolution of Al, the anodic potentiostatic polarization tests are performed at −0.7 V (vs SCE). Figure 10 shows the potentiostatic polarization curves of specimens after 24 h of testing under various test conditions in 3.5 wt.% NaCl solution containing *A. terreus*. For the control specimen, the anodic current density in the presence of *A. terreus* is the largest, suggesting that *A. terreus* can significantly accelerate the corrosion of the specimen without applying any corrosion control strategies. The anodic current densities of specimens in the presence of UV radiation and BKC are close, and it is slightly high in the presence of BKC. This indicates that the single use of UV radiation and BKC has an inhibition effect against the fungi corrosion caused by *A. terreus*. When UV radiation and BKC are present simultaneously, the anodic current density is the smallest, demonstrating that the combination of UV radiation and BKC can effectively inhibit the anodic dissolution caused by *A. terreus*, and they have a synergistic corrosion inhibition behavior. These results are also in accordance with the above experimental results, such as EIS data (Figs. 6 and 8) and polarization curves (Fig. 9).

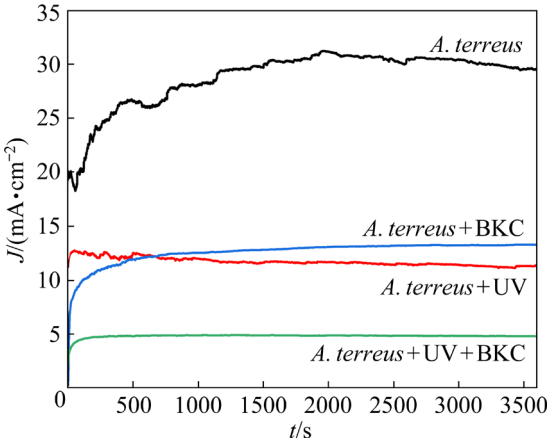


**Fig. 10** Potentiostatic polarization curves of specimens in the presence of *A. terreus* after 24 h of testing under different test conditions in 3.5 wt.% NaCl solution

## 4 Discussion

The bare surface morphologies after removing biofilm (Fig. 3), EIS data (Figs. 6 and 8), as well as potentiodynamic and potentiostatic polarization curves (Figs. 9 and 10), have confirmed that fungus *A. terreus* has a good ability to distinctly accelerate AA corrosion, and severe pitting corrosion can also be induced. The corrosion acceleration of AA derives from the good growth and metabolic activity of *A. terreus* (Fig. 1) as well as the subsequent biofilm formation on the specimens, because the existence of large amounts of hyphae and spores is found (Figs. 2(a) and (b)). Fungi like to grow and keep good metabolic activity in humid marine environments [35,36]. The previous

studies [7,11,12,28] also verified that fungal *Aspergillus* as one of the corrosive microorganisms could significantly accelerate AA corrosion through direct or indirect electron transfer as well as their metabolic products, such as organic acids. In addition, the pitting susceptibility of AA is connected with the nature of its passive film. Therefore, the formation of pitting corrosion suggests that *A. terreus* can cause local damage to the AA passive film. As a result, it is reasonable that *A. terreus* promotes the corrosion acceleration of AA specimens.

The control of fungal-induced corrosion is essential. When UV radiation is applied, it is found that the planktonic and sessile spores of *A. terreus* both decline by about an order of magnitude in comparison to those of the control (Fig. 1). Furthermore, SEM images (Figs. 2(d) and (e)) show that small amounts of hyphae and spores get together, which means that UV radiation surely can inhibit the biological activity of *A. terreus*. The decrease of the growth of *A. terreus* especially for the sessile spores can surely slow down AA corrosion. On the other hand, direct UV radiation also can influence AA corrosion. UV radiation can change the structure of passive film leading to the increase of passive film, stability as well as the decrease of AA corrosion, and the incident photons can inhibit the initiation of pitting corrosion [24,37,38]. Therefore, the corrosion of AA specimens caused by *A. terreus* should decrease due to the action of UV radiation. And for the fungal-induced corrosion of AA, UV radiation can be a good and effective method. But long-term radiation can cause the genovariation of *A. terreus*, increasing their adaptability, and then leading to the decline of the protective effect of UV radiation.

Except for UV radiation, BKC with a concentration of 20 mg/L is also used to control fungal-induced corrosion. Similarly, BKC as a biocide can inhibit the growth of *A. terreus*, leading to the decrease of spore counts (Fig. 1). Some spores can still be found on the surface of the specimen. Therefore, the application of BKC can also inhibit the biological activity of *A. terreus*. Previous reports [39−43] have indicated that BKC can directly or indirectly inhibit or kill bacteria, fungi, and algae. As discussed above, the decrease of biological activity of *A. terreus* caused by BKC should also result in the mitigation of AA corrosion. The surface morphologies (Fig. 3) and electrochemical measurements (Figs. 6 and 8−10) also confirm the mitigation of AA corrosion caused by BKC. In addition, BKC can inhibit biological activity and metal corrosion as a corrosion inhibitor [27,42]. The adsorption of BKC on specimens can significantly inhibit the attachment of *A. terreus* as well as the subsequent formation of biofilm. XPS results also confirm the adsorption of BKC on specimens due to the appearance of C—N functional group (Fig. 4(e)). Therefore, only a few spores can be seen on specimens (Figs. 2(g) and (h)). However, the coverage ratio of BKC on the specimen surface as well as the germicidal efficiency depends on the used concentration of BKC. The BKC of 20 mg/L cannot satisfy the requirements of good disinfection and corrosion inhibition effects. Therefore, BKC of 20 mg/L can only partly inhibit AA corrosion induced by *A. terreus*, but the corrosion inhibition effect is not ideal (Figs. 8 and 10).

From the discussion above, it is seen that the single use of UV radiation or BKC can inhibit AA corrosion induced by *A. terreus* but the corresponding corrosion inhibition efficiencies are not ideal due to the low intensity of UV radiation and the low concentration of BKC. However, the combination of UV radiation and BKC can be a good strategy to control fungal-induced corrosion of AA. The experimental results, such as surface morphologies (Fig. 3), EIS data (Figs. 6 and 8), potentiodynamic and potentiostatic polarization curves (Figs. 9 and 10), demonstrate that the combined application of UV radiation and BKC has a synergistic corrosion inhibition effect for AA in the presence of *A. terreus* due to the fast decrease of corrosion rate compared to the single use of UV radiation or BKC. The synergistic corrosion inhibition of UV radiation and BKC can come from two aspects. Firstly, the simultaneous application of UV radiation and BKC has caused a fast decrease of the planktonic and sessile spores of *A. terreus*. The decrease of biological activity of *A. terreus* makes a decrease in the corrosivity of *A. terreus* against, thus then cause slight corrosion of AA. Secondly, both the UV radiation and BKC can inhibit the abiotic corrosion of AA as shown above. This means that the protective efficacy of AA passive film can be also enhanced under the actions of UV radiation and BKC. Therefore, the

combination of UV radiation and BKC should have a synergistic action to inhibit AA corrosion from the abiotic aspect. As a result, the corrosion of AA can be effectively inhibited by UV radiation and BKC, and almost no corrosion pits are seen (Figs. 3(g) and (h)). Therefore, the combined application of UV radiation and BKC can be a good method to effectively inhibit the fungal-induced corrosion of AA. The UV radiation of low intensity, as well as BKC of low concentration, can avoid their potential damage to natural environments.

## 5 Conclusions

(1) *A. terreus* can maintain good biological activity in the test solution and the planktonic spore count of *A. terreus* is $7.7\times10^7$ spores/mL after 21 d of testing. The application of UV radiation and BKC effectively inhibits the growth of *A. terreus*, leading to the decline of fungal biological activity. The antifungal effect of BKC is better than that of UV radiation when they are singly used.

(2) The sessile and planktonic spore counts of *A. terreus* are $5.4\times10^5$ spores/cm$^2$ and $1.0\times10^5$ spores/mL after 21 d of testing when UV radiation and BKC are combinedly used. Therefore, the combination of UV and BKC has a synergistic antifungal effect for *A. terreus*, and inhibits the attachment of *A. terreus* on AA as well as the formation of biofilm.

(3) *A. terreus* can seriously accelerate AA corrosion, and a large biogenetical corrosion pit can be found. The primary fungal-induced corrosion products of AA are $Al(OH)_3$ and $Al_2O_3$. The individual use of UV radiation or BKC can inhibit the AA corrosion induced by *A. terreus*, but a small number of corrosion pits can still be observed. The corrosion inhibition behavior of UV radiation and BKC is different. Therefore, the corrosion inhibition effect of UV radiation or BKC is not ideal when they are individually applied. However, no recognized corrosion pits can be found when UV radiation and BKC are combinedly used.

(4) Electrochemical measurements also confirm that the combination of UV radiation and BKC has a higher corrosion inhibition efficiency for AA in the presence of *A. terreus*. Potentiostatic polarization curves demonstrate that the current density of the specimen decreases by about one order of magnitude when UV radiation and BKC are applied simultaneously in comparison to that of the control specimen. Therefore, it is concluded that the combination of UV radiation and BKC has a synergistic inhibition effect on AA corrosion induced by *A. terreus*. Furthermore, the simultaneous implementation of UV radiation and BKC can avoid the potential damage of UV radiation and BKC to natural environments due to their low intensity or concentration.

### CRediT authorship contribution statement

**Zheng-yu JIN:** Conceptualization, Investigation, Writing − Original draft; **Chao WANG:** Investigation, Data curation, Validation; **Hai-xian LIU:** Formal analysis, Visualization; **Hong-wei LIU:** Conceptualization, Formal analysis, Writing − Review & editing, Supervision, Funding acquisition.

### Declaration of competing interest

The authors declare that they have no known competing financial interests or personal relationships that could have appeared to influence the work reported in this paper.

### Acknowledgments

This work was supported by the Guangdong Basic and Applied Basic Research Foundation, China (No. 2023A1515012146), the National Natural Science Foundation of China (No. 52271083), the Fundamental Research Funds for the Central Universities, China (No. 22qntd0801), and the Shanghai Engineering Technology Research Centre of Deep Offshore Material, China (No. 19DZ2253100).

### References

[1] LIU Peng, HU Jia-ying, LI Huai-xue, SUN Si-yu, ZHANG Yuan-bin. Effect of heat treatment on microstructure, hardness and corrosion resistance of 7075 Al alloys fabricated by SLM [J]. Journal of Manufacturing Processes, 2020, 60: 578−585.

[2] XIE Peng, CHEN Song-yi, CHEN Kang-hua, JIAO Hui-bin, HUANG Lan-ping, ZHANG Zhuo, YANG Zhen. Enhancing the stress corrosion cracking resistance of a low-Cu containing Al−Zn−Mg−Cu aluminum alloy by step-quench and aging heat treatment [J]. Corrosion Science, 2019, 161: 108184.

[3] JI Yuan-yuan, XU Yun-ze, ZHANG Bin-bin, BEHNAMIAN Y, XIA Da-hai, HU Wen-bin. Review of micro-scale and atomic-scale corrosion mechanisms of second phases in aluminum alloys [J]. Transactions of Nonferrous Metals Society of China, 2021, 31: 3205−3227.

[4] LIU Fang, ZHENG Jing-xu, CHEN Xia, XU Xue-song,

CHEN Bin. Study on corrosion resistance of artificially aged 7075 aluminium alloy by using Cs-corrected STEM [J]. Transactions of Nonferrous Metals Society of China, 2022, 32: 2828−2837.

[5] ZHAO Qi-yue, GUO Chuang, NIU Ke-ke, ZHAO Jin-bin, HUANG Yun-hua, LI Xiao-gang. Long-term corrosion behavior of the 7A85 aluminum alloy in an industrial-marine atmospheric environment [J]. Journal of Materials Research and Technology, 2021, 12: 1350−1359.

[6] LÓPEZ FREIXES M, ZHOU Xu-yang, ZHAO Huan, GODIN H, PEGUET L, WARNER T, GAULT B. Revisiting stress-corrosion cracking and hydrogen embrittlement in 7xxx Al alloys at the near-atomic-scale [J]. Nature Communications, 2022, 13: 1−9.

[7] ZHANG Tian-sui, WANG Jun-lei, ZHANG Guo-an, LIU Hong-fang. The corrosion promoting mechanism of *Aspergillus niger* on 5083 aluminum alloy and inhibition performance of miconazole nitrate [J]. Corrosion Science, 2020, 176: 108930.

[8] GUAN Fang, ZHAI Xiao-fan, DUAN Ji-zhou, ZHANG Jie, LI Ke, HOU Bao-rong. Influence of sulfate-reducing bacteria on the corrosion behavior of 5052 aluminum alloy [J]. Surface and Coatings Technology, 2017, 316: 171−179.

[9] ZHANG Jie, WANG Jia, ZHANG Bin-bin, ZENG Yu-xiang, DUAN Ji-zhou, HOU Bao-rong. Fabrication of anodized superhydrophobic 5083 aluminum alloy surface for marine anti-corrosion and anti-biofouling [J]. Journal of Oceanology and Limnology, 2020, 38: 1246−1255.

[10] SMIRNOV V F, BELOV D V, SOKOLOVA T N, KUZINA O V, KARTASHOV V R. Microbiological corrosion of *aluminum alloys* [J]. Applied Biochemistry and Microbiology, 2008, 44: 192−196.

[11] JIRON-LAZOS U, CORVO F, ROSA S C, GARCIA-OCHOA E M, BASTIDAS D M, BASTIDAS J M. Localized corrosion of aluminum alloy 6061 in the presence of *Aspergillus niger* [J]. International Biodeterioration and Biodegradation, 2018, 133: 17−25.

[12] ZHANG Yu-xuan, HE Jia-qi, ZHENG Li, JIN Zheng-yu, LIU Hai-xian, LIU Lan, GAO Zhi-zeng, MENG Guo-zhe, LIU Hong-fang, LIU Hong-wei. Corrosion of aluminum alloy 7075 induced by marine *Aspergillus terreus* with continued organic carbon starvation [J]. NPJ Materials Degradation, 2022, 6: 1−12.

[13] WANG Jun-lei, XIONG Fu-ping, LIU Hong-wei, ZHANG Tian-sui, LI Yan-yan, LI Chen-jing, XIA Wu, WANG Hai-tao, LIU Hong-fang. Study of the corrosion behavior of *Aspergillus niger* on 7075-T6 aluminum alloy in a high salinity environment [J]. Bioelectrochemistry, 2019, 129: 10−17.

[14] XU Jin, JIA Ru, YANG Dong-qing, SUN Cheng, GU Ting-yue. Effects of D-phenylalanine as a biocide enhancer of THPS against the microbiologically influenced corrosion of C1018 carbon steel [J]. Journal of Materials Science & Technology, 2019, 35: 109−117.

[15] WANG Jun-lei, HOU Bao-shan, XIANG Jun, CHEN Xue-dong, GU Ting-yue, LIU Hong-fang. The performance and mechanism of bifunctional biocide sodium pyrithione against sulfate reducing bacteria in X80 carbon steel corrosion [J]. Corrosion Science, 2019, 150: 296−308.

[16] PINNOCK T, VOORDOUW J, VOORDOUW G. Use of carbon steel ball bearings to determine the effect of biocides and corrosion inhibitors on microbiologically influenced corrosion under flow conditions [J]. Applied Microbiology and Biotechnology, 2018, 102: 5741−5751.

[17] JIA R, UNSAL T, XU D K, LEKBACH Y, GU T Y. Microbiologically influenced corrosion and current mitigation strategies: A state of the art review [J]. International Biodeterioration & Biodegradation, 2019, 137: 42−58.

[18] XU Li-ting, GUAN Fang, MA Yan, ZHANG Rui-yong, ZHANG Yi-meng, ZHAI Xiao-fan, DONG Xu-cheng, WANG Ya-nan, DUAN Ji-zhou, HOU Bao-rong. Inadequate dosing of THPS treatment increases microbially influenced corrosion of pipeline steel by inducing biofilm growth of *Desulfovibrio hontreensis* SY-21 [J]. Bioelectrochemistry, 2022, 145: 108048.

[19] LAMIN A, KAKSONEN A H, COLE I S, CHEN X B. Quorum sensing inhibitors applications: A new prospect for mitigation of microbiologically influenced corrosion [J]. Bioelectrochemistry, 2022, 145: 108050.

[20] LI Ying-chao, JIA Ru, AL-MAHAMEDH H H, XU Da-ke, GU Ting-yue. Enhanced biocide mitigation of field biofilm consortia by a mixture of D-amino acids [J]. Frontiers in Microbiology, 2016, 7: 896.

[21] YANG Shi-wen, DU Xiao-sheng, DENG Sha, QIU Jing-hong, DU Zong-liang, CHENG Xu, WANG Hai-bo. Recyclable and self-healing polyurethane composites based on Diels−Alder reaction for efficient solar-to-thermal energy storage [J]. Chemical Engineering Journal, 2020, 398: 125654.

[22] SANTOS A L, OLIVERIA V, BAPTISTA I, HENRIQUES I, GOMES N C M, ALMEIDA A, CORREIA A, CUNHA Â. Wavelength dependence of biological damage induced by UV radiation on bacteria [J]. Archives of Microbiology, 2013, 195: 63−74.

[23] SINGH H, BHARDWAJ S K, KHATRI M, KIM K H, BHARDWAJ N. UVC radiation for food safety: An emerging technology for the microbial disinfection of food products [J]. Chemical Engineering Journal, 2021, 417: 128084.

[24] AMIN M A. Uniform and pitting corrosion events induced by SCN: Anions on Al alloys surfaces and the effect of UV light [J]. Electrochimica Acta, 2011, 56: 2518−2531.

[25] WU Jin-xian, WANG Ju-lin. The effects of UV and visible light on the corrosion of bronze covered with an oxide film in aqueous solution [J]. Corrosion Science, 2019, 154: 144−158.

[26] MACHUCA L L, JEFFREY R, BAILEY S I, GUBNER R, WATKIN E L J, GINIGE M P, KAKSONEN A H, HEIDERSBACH K. Filtration–UV irradiation as an option for mitigating the risk of microbiologically influenced corrosion of subsea construction alloys in seawater [J]. Corrosion Science, 2014, 79: 89−99.

[27] LIU Hong-wei, GU Ting-yue, LV Ya-lin, ASIF M, XIONG Fu-ping, ZHANG Guo-an, LIU Hong-fang. Corrosion inhibition and anti-bacterial efficacy of benzalkonium chloride in artificial $CO_2$-saturated oilfield produced water [J]. Corrosion Science, 2017, 117: 24−34.

[28] ZHANG Yu-xuan, LIU Hai-xian, JIN Zheng-yu, LAI Huan-sheng, LIU Hong-fang, LIU Hong-wei. Fungi corrosion of high-strength aluminum alloys with different microstructures caused by marine *Aspergillus terreus* under seawater drop [J]. Corrosion Science, 2023, 212: 110960.
[29] DAI Xin-yan, WANG Hua, JU L K, CHENG Gang, CONG Hong-bo, NEWBY B M Z. Corrosion of aluminum alloy 2024 caused by *Aspergillus niger* [J]. International Biodeterioration and Biodegradation, 2016, 115: 1−10.
[30] HSIAO H Y, TSAI W T. Characterization of anodic films formed on AZ91D magnesium alloy [J]. Surface and Coatings Technology, 2005, 190: 299−308.
[31] BAJAT J B, MILOSEV I, JOVANOVIC Ž, MISKOVIC-STANKOVIC V B. Studies on adhesion characteristics and corrosion behaviour of vinyltriethoxysilane/ epoxy coating protective system on aluminium [J]. Applied Surface Science, 2010, 256: 3508−3517.
[32] PRAKASHAIAH B G, VINAYA KUMARA D, ANUP PANDITH A, NITYANANDA SHETTY A, AMITHA RANI B E. Corrosion inhibition of 2024-T3 aluminum alloy in 3.5% NaCl by thiosemicarbazone derivatives [J]. Corrosion Science, 2018, 136: 326−338.
[33] ZHANG Bo, ZHOU Hai-bo, HAN En-hou, KE Wei. Effects of a small addition of Mn on the corrosion behaviour of Zn in a mixed solution [J]. Electrochimica Acta, 2009, 54: 6598−6608.
[34] LI Xue-wu, YAN Jia-yang, YU Teng, ZHANG Bin-bin. Versatile nonfluorinated superhydrophobic coating with self-cleaning, anti-fouling, anti-corrosion and mechanical stability [J]. Colloids and Surfaces A: Physicochemical and Engineering Aspects, 2022, 642: 128701.
[35] JONES E, RAMAKRISHNA S, VIKINESWARY S, DAS D, BAHKALI A, GUO Sheng-yu, PENG Ka-lai. How do fungi survive in the sea and respond to climate change? [J]. Journal of Fungi, 2022, 8: 291.
[36] SINGH P, RAGHUKUMAR C, VERMA P, SHOUCHE Y. Phylogenetic diversity of culturable fungi from the deep-sea sediments of the Central Indian Basin and their growth characteristics [J]. Fungal Diversity, 2010, 40: 89−102.
[37] MOUSSA S O, HOCKING M G. The photo-inhibition of localized corrosion of 304 stainless steel in sodium chloride environment [J]. Corrosion Science, 2001, 43: 2037−2047.
[38] LENHART S, URQUIDI-MACDONALD M, MACDONALD D D. Photo-inhibition of passivity breakdown on nickel [J]. Electrochimica Acta, 1987, 32: 1739−1741.
[39] HOUARI A, DI MARTINO P. Effect of chlorhexidine and benzalkonium chloride on bacterial biofilm formation [J]. Letters in Applied Microbiology, 2007, 45: 652−656.
[40] RODRIGUEZ-LOPEZ P, CARBALLO-JUSTO A, DRAPER L, CABO M L. Removal of Listeria monocytogenes dual-species biofilms using combined enzyme-benzalkonium chloride treatments [J]. Biofouling, 2017, 33: 45−58.
[41] SANMARTIN P, RODRIGUEZ A, AGUIAR U. Medium-term field evaluation of several widely used cleaning-restoration techniques applied to algal biofilm formed on a granite-built historical monument [J]. International Biodeterioration & Biodegradation, 2020, 147: 104870.
[42] WANG Jun-lei, ZHANG Tian-sui, ZHANG Xin-xin, ASIF M, JIANG Li-pei, DONG Shuang, GU Ting-yue, LIU Hong-fang. Inhibition effects of benzalkonium chloride on Chlorella vulgaris induced corrosion of carbon steel [J]. Journal of Materials Science and Technology, 2020, 43: 14−20.
[43] STUPAR M, GRBIC M L, DZAMIC A, UNKOVIC N, RISTIC M, JELIKIC A, VUKOJEVIC J. Antifungal activity of selected essential oils and biocide benzalkonium chloride against the fungi isolated from cultural heritage objects [J]. South African Journal of Botany, 2014, 93: 118−124.

# 紫外辐射和杀菌剂组合对高强 7075 铝合金霉菌腐蚀的影响

金正宇，王 超，柳海宪，刘宏伟

中山大学 化学工程与技术学院，珠海 519082

**摘 要**：通过生物活性分析、表面分析和电化学测量等方法，深入研究紫外辐射和杀菌剂苯扎氯铵对由土曲霉引起的高强 7075 铝合金真菌腐蚀的影响。与对照组相比，当紫外辐射和苯扎氯铵联合使用时，附着在材料表面的孢子浓度和溶液中浮游孢子浓度均下降了两个数量级以上。紫外辐射可抑制霉菌的生物活性，影响铝合金钝化膜的稳定性。除直接杀菌外，苯扎氯铵在材料表面的物理吸附可以有效抑制霉菌的附着。紫外辐射和苯扎氯铵的联合使用通过协同作用，可以更有效地抑制铝合金的腐蚀，尤其是点蚀。因此，紫外辐射和苯扎氯铵的联合使用可作为一种良好的方法有效抑制真菌腐蚀。

**关键词**：真菌腐蚀；土曲霉；7075 铝合金；紫外辐射；苯扎氯铵

**(Edited by Wei-ping CHEN)**